frontiers | Frontiers in Earth Science

TYPE Original Research
PUBLISHED 01 September 2022
DOI 10.3389/feart.2022.905940

OPEN ACCESS

EDITED BY
Yan Du,
University of Science and Technology Beijing, China

REVIEWED BY
Eleyas Assefa,
Addis Ababa University, Ethiopia
Biao Hu,
Shenzhen University, China
Qingxiang Meng,
Hohai University, China

*CORRESPONDENCE
Deng Huafeng,
dhf8010@ctgu.edu.cn

SPECIALTY SECTION
This article was submitted to Earth and Planetary Materials, a section of the journal Frontiers in Earth Science

RECEIVED 29 March 2022
ACCEPTED 05 August 2022
PUBLISHED 01 September 2022

CITATION
Yao X, Huafeng D, Jianlin L and Xingzhou C (2022), Shear performance and reinforcement mechanism of MICP-treated single fractured sandstone. *Front. Earth Sci.* 10:905940. doi: 10.3389/feart.2022.905940

Shear performance and reinforcement mechanism of MICP-treated single fractured sandstone

Xiao Yao[1], Deng Huafeng[1]*, Li Jianlin[1] and Chen Xingzhou[2]

[1]Key Laboratory of Geological Hazards on Three Gorges Reservoir Area, Ministry of Education, College of Civil Engineering and Architecture, China Three Gorges University, Yichang, Hubei, China, [2]College of Architecture and Civil Engineering, Xi'an University of Science and Technology, Xi'an, Shanxi, China

There are a large number of fractured rock masses in the Three Gorges Reservoir area. Traditional reinforcement methods have disadvantages such as large engineering investment, high material consumption, and poor ecological environmental protection. Therefore, it is necessary to develop new environmentally friendly materials and methods to strengthen and control them. The microbial-induced carbonate precipitation (MICP) technology that has emerged in recent years has the characteristics of low carbon and environmental protection and has great prospects in the restoration and reinforcement of rock and soil materials. Therefore, *Bacillus cereus* extracted *in situ* from the Three Gorges Reservoir area is proposed to be used for MICP reinforcement of single-fractured sandstone, and its reinforcement mechanism is revealed by studying the macroscopic impermeability and shear performance improvement of the fractured rock sample after reinforcement, and the microstructure changes. The results show that after 10 cycles of grouting reinforcement, the fracture surface of the rock sample is well sealed, the permeability coefficient is reduced by two orders of magnitude, the shear stress is increased by 26%–40%, and the shear stiffness is increased by 70%. The shear stress–shear displacement curve shows the peak shear strength, and the residual shear strength also increases to a certain extent. The MICP process improves the mechanical properties of fractured rock samples from three aspects, namely, the cementation between sand grains and the fracture surface, the cementation effect between sand grains, and the filling effect of fractured rock samples. The shear failure surface of the samples after reinforcement is the recheck interface between the cementation body and the cementation interface. The relevant research results can provide references for the MICP reinforcement technology of fractured rock mass.

KEYWORDS

fractured sandstone, MICP, shear stress, racture surface filling, reinforcement mechanism

Introduction

The rock mass on the bank slope often has a large number of microscopic or macroscopic defects such as bedding, joints, and fissures. The existence of defects in the rock mass greatly affects the stress field, seepage field, and chemical field inside the rock mass structure (Miao et al., 2018; Wang et al., 2021). It often controls the stability of the entire rock mass structure, and once instability occurs, the resulting disaster will be catastrophic (Du et al., 2021). Therefore, the reinforcement and treatment of the fractured rock mass is a necessary means to prevent the occurrence of disasters. At present, the main prevention methods mainly include bolt reinforcement (Zhu et al., 2018), prestressed anchor cable reinforcement (Jiang et al., 2019), chemical grouting reinforcement (Benmokrane et al., 1996), and anti-sliding pile reinforcement (Zhu et al., 2021). These reinforcement measures can improve the mechanical properties of fractured rock mass to a certain extent and reduce the possibility of disasters. There are also disadvantages such as high energy consumption, high pollution emissions, high cost, and poor durability. With the proposal of environmental protection goals such as "3060 Dual-Carbon Target" and "Yangtze River Protection," it is urgent to research and develop new reinforcement methods to meet better environmental compatibility on the basis of saving economic costs. Among them, the reinforcement technology based on MICP technology (Dejong et al., 2006) is one of the main directions researchers in related fields pay attention to. The essence of MICP technology is to use urease secreted by mineralizing microorganisms to hydrolyze urea to generate carbonate radicals in an alkaline environment and combine with calcium ions adsorbed by negatively charged microorganisms to form cemented calcium carbonate crystals, thereby filling pore materials. They stick together to form a solidified body with a certain strength (Rong et al., 2011; Liu et al., 2020).

With the in-depth study of MICP technology, it has made great progress in the field of geotechnical engineering, such as sand foundation reinforcement (Whiffin et al., 2007; Gomez et al., 2019; Touhidul et al., 2020), earthquake liquefaction prevention (Han et al., 2016; Montoya et al., 2013; Paassen et al., 2010), sand dust control (Li et al., 2017), and erosion protection (Cheng et al., 2013; Chen et al., 2016; Jiang and Soga, 2017; Tian et al., 2018). Relevant researchers have made a lot of achievements in rock and soil reinforcement, but the research on microbial reinforcement of fractured rock mass is still in the initial stage. It was found that the permeability coefficient of fractured limestone can be reduced to the order of 10^{-6} cm/s by using a microbial grouting technique (Zhi et al., 2019). Li (2019) also used this method to reinforce cracked granite and sandstone samples under different filling medium conditions and he found that the filling medium was favorable for carbonate precipitation and reinforcing the rock fractures. Deng et al. (2019) used *Sporosarcina pasteurii* to repair fractured yellow sandstone samples, and the microbial process could cement the fillings and samples and greatly reduce the porosity. After MICP reinforcement of two different types of sandstone, Song et al. (2022) found that although the quality of $CaCO_3$ precipitated over time in the two rock types was similar, the unconfined compressive strength of low-strength sandstone increased significantly and its mechanical properties are divided into three distinct stages, while there is no significant improvement in the mechanical properties of high-strength sandstone. Zou et al. (2021) conducted four groups of seepage experiments on transparent rock samples filled with MICP, and studied the effects of bacterial concentration, crack inclination angle, crack roughness, and crack opening on fracture permeability. The results show that the fracture permeability of MICP-filled fractures increases with the increase of crack inclination, roughness, and opening; it first increases and then decreases. At the same time, the shape of the crack has a certain influence on the filling method of calcium carbonate and it needs to be properly considered in engineering practice. These research results laid a good foundation for MICP reinforcement of fractured rock mass, but they mainly focus on the impermeability or the tensile strength/unconfined compressive strength of fractured rock mass; there are few research studies on the shear behavior of reinforced fractured rock mass. The deformation and failure of engineering rock mass are often controlled by the strength of joints, cracks, and other structural planes. Engineering practice has repeatedly proved that the instability of rock mass is mostly due to the shear failure of weak structural planes.

On this basis, this study intends to use MICP technology to strengthen single fractured sandstone. First, the fractured rock samples were reinforced with *in situ B. cereus* for 10 strengthening cycles. After that, by comparing the physical and mechanical properties of the samples before reinforcement, the effect of MICP reinforcement technology on the impermeability and shear resistance of the fractured samples was studied. The improvement effect, combined with the changes in the micro-structure before and after reinforcement, preliminarily revealed the mechanism of microbial reinforcement of fractured rock mass and provided reference and ideas for the research and application of microbial reinforcement of fractured rock mass.

Materials and methods

Self-extracted bacteria of *B. cereus*

At present, under different environmental conditions, the urease activity of the commonly used carbonate-mineralization microbe (such as *Sporosarcina pasteurii*, *Bacillus pasteuris*, etc.) is different, and the survival adaptability of bacteria in different

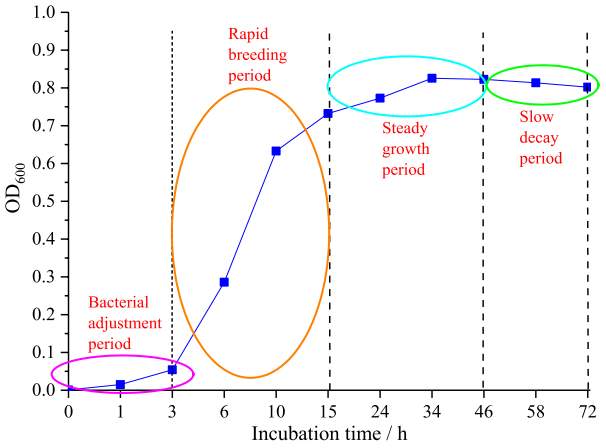

FIGURE 1
Growth curve of Bacillus cereus under the culture condition.

fields is uncertain. In recent years, some researchers have turned to isolate the bacteria in different environmental conditions, and their results show that the *in situ* microorganisms can be used to reinforce the corresponding materials and the reinforcement effect is better (Qian et al., 2010; Khan et al., 2015; Li et al., 2019). Hence, the *in situ* extracted *B. cereus* is used to reinforce the fractured samples in the Three Gorges Reservoir area.

The culture condition of *B. cereus* is as follows: urea 40 g/L, peptone 10 g/L, beef extract 3 g/L, and NaCl 5 g/L. The bacterial inoculation volume is 2.0 ml per 100 ml liquid medium. After inoculation, the medium is placed in a shaker for 72 h at 30°C, and the rotation speed of the rocker is 180 r/min. During the cultivation process, the concentration of the bacterial solution was measured at regular intervals; OD_{600} is used to characterize the concentration, which is the absorbance of the solution at a wavelength of 600 nm. The growth curve of *B. cereus* is shown in Figure 1.

Preparation of a single fracture sandstone sample

It is difficult to collect naturally fractured rock mass on site, so we used the artificial joint preparation method to prepare the samples (Zhang et al., 2022). A standard cube sample with a length of 100 mm was made by cutting and grinding to avoid damage at the edges according to Li et al. (2022) (Figure 2A), and then the samples were split along the layered weak surface from the middle of the samples (Figure 2B). They were selected with a flat joint surface and no local block as the single fractured samples for reinforcement. The typical single fractured sample is shown in Figure 2C; the red arrow indicates the shear direction.

To accurately find out the reinforcement effect on the shear strength of the samples, it is necessary to obtain the

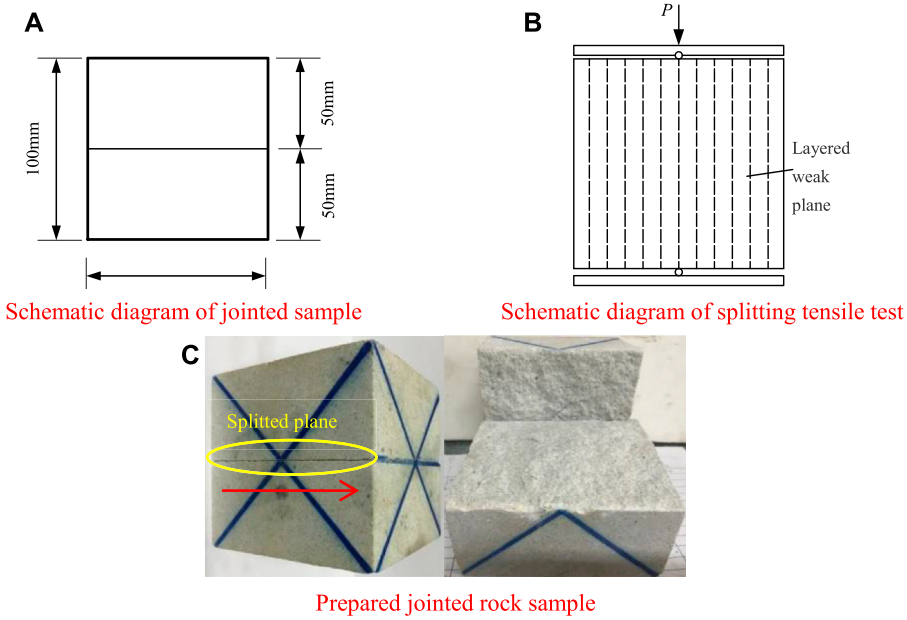

FIGURE 2
Typical single fractured sample.

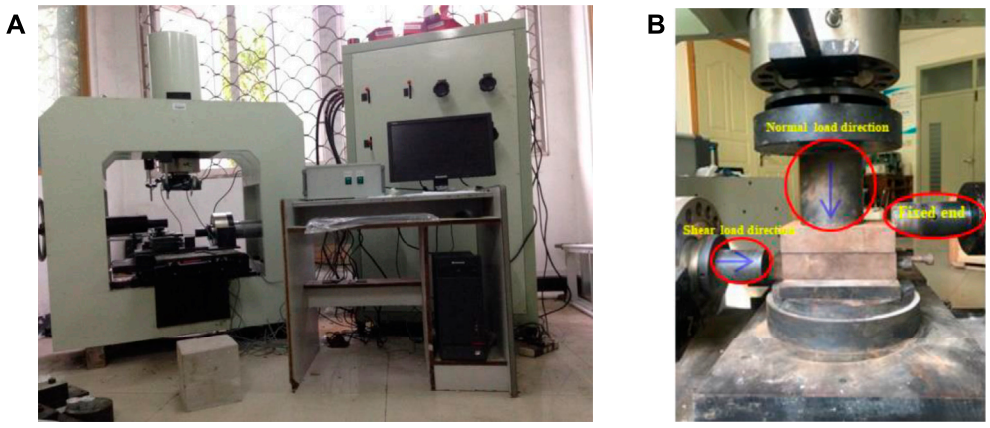

FIGURE 3
Shear test device.

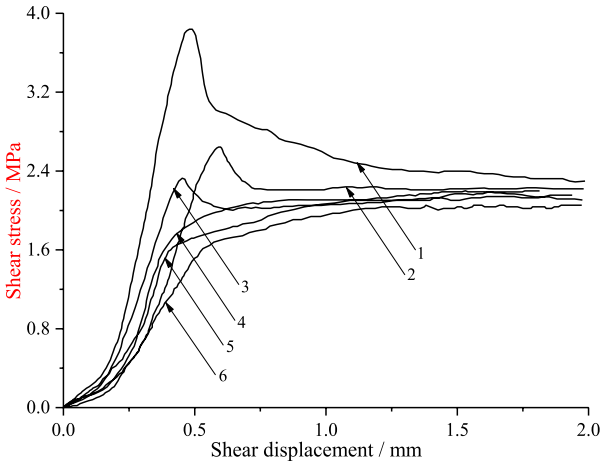

FIGURE 4
Shear stress–shear displacement curves of the sample under repeated shear tests (taking one sample under 2.0 MPa as an example).

shear strength of the samples before reinforcement. According to our previous study of fractured sandstone, we found that the shear mechanical properties of the fractured surface decrease gradually with the increase of shearing times (Deng et al., 2018). Therefore, the single fractured samples were subjected to repeated shear tests under four kinds of different normal stresses, namely, 1.0, 1.5, 2.0, and 2.5 MPa. A total of three samples were prepared under each normal stress and the test was carried out on the shear testing device (as shown in Figure 3). The loading process of the specimen is as follows. After the sample is loaded into the shear box, the normal preload is first performed to ensure that the normal pressure probe is in good contact with the shear box; then the normal load is applied (e.g., 1.0, 1.5, 2.0, and 2.5 MPa), followed by tangential preloading, which is to fix the upper shear box; finally, the tangential load is applied until the shear stress–strain curve shows a peak intensity and reaches a steady state. The shear stress–shear displacement curve of a typical fracture sample under repeated shear action is shown in Figure 4. The shear stress of the fractured sample tended to be stable after five or six shear times, so the shear stress of the sixth time was taken as the shear stress of the samples before reinforcement.

Grouting reinforcement process

A total of 10 cycles of reinforcement of the grouting process were designed. The grouting environment temperature was 25°C ± 1°C and the humidity was about 40%. The OD_{600} value of the bacterial solution was about 0.8. Previous studies had shown that the addition of NH_4Cl and $NaHCO_3$ in the grouting process can improve the alkalinity of the solution environment and make urease show higher activity and stronger affinity (Ahmed et al., 2012; Zhao et al., 2014). Therefore, a certain concentration of NH_4Cl solution and $NaHCO_3$ solution was added to the cementation solution and then injected into the single fractured sample to enhance the reinforcement effect. The types and proportions of solutions required in the reinforcement process are shown in Supplementary Table S1

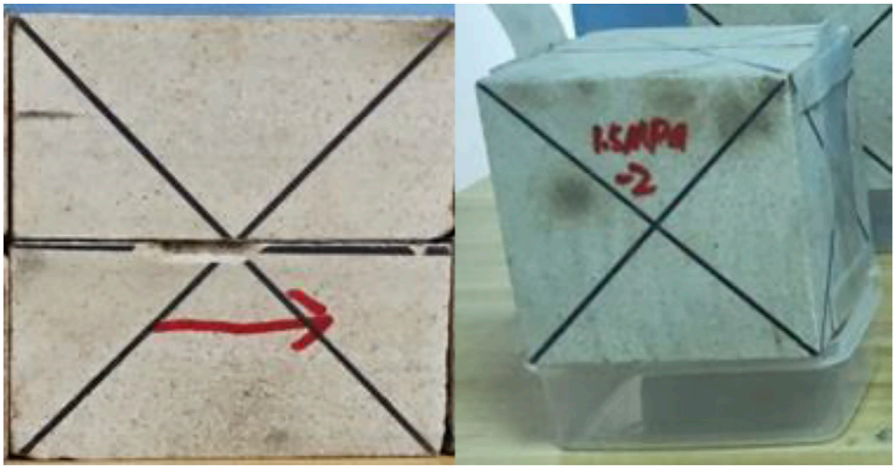

FIGURE 5
Typical single fractured samples.

Referring to the previous experiment (Rong et al., 2012; Zhang et al., 2015) and combined with the characteristics of the single fractured samples, the grouting steps were designed as follows:

1) Cleaning the debris on the fracture surface of the samples, washing the samples with distilled water, soaking for 24 h, and drying for standby.
2) Justifying the upper and lower plates of the samples, bonding the samples from the side with silicon adhesive tape, and controlling the average width of the fractured surface to be 1 mm at the same time. To enhance the reinforcement effect, standard quartz sand was filled in the fracture according to the idea of Li et al. (2019). Silicone adhesive tape had two functions: one was to maintain the crack width of the sample; the other was to prevent the grouting solution from flowing out from the side of the samples, so as not to weaken the reinforcement effect. Typical samples before strengthening are shown in Figure 5.
3) Dripping 10 ml of fixation solution into the cracks slowly and evenly from the top of the samples.
4) Dripping 20 ml of bacterial solution into the cracks and standing for 2 h to ensure full diffusion and adsorption of bacteria on the fractured surface of the samples and in the filled sand.
5) Fully mixing 30 ml 0.5 mol/L cementation solution, 10 ml 0.1 mol/L NH_4Cl solution, and 10 ml 0.1 mol/L $NaHCO_3$ solution together, and then dripping the mixture into the fracture slowly and uniformly, standing for 12 h (Chu et al., 2012).

Steps 3–5 were collectively referred to as one grouting process. After standing for 10 h, the second grouting process was carried out. Based on this, a total of 10 cyclic processes were carried out for 10 days. Then the samples were put into an oven at a temperature of 60°C. After drying to a constant weight, the shear test of the reinforced samples was performed.

The typical samples of fractured surfaces after reinforcement are shown in Figure 6. The macroscopic physical and mechanical tests of constant head seepage and different normal stresses were carried out on the samples. Combined with microscopic analysis methods, the calcium carbonate deposition state and reinforcement mechanism were analyzed in detail.

Results and discussion

Constant head seepage test

The self-made constant head seepage device is used to measure the flow of single fractured samples before and after reinforcement as shown in Figure 7. The permeability coefficient is calculated according to Eq. 1:

$$k = \frac{QL}{A\mathrm{t}\Delta\mathrm{h}} \tag{1}$$

In the equation, k is the permeability coefficient; Q is the fluid flow; t is the measurement time; A is the cross-sectional area; L is the length; and Δh is the high difference at both ends of the sample.

Calculating by Eq. 1, the order of magnitude of the permeability coefficient before reinforcement is about 10^{-5} m/s and after reinforcement is about 10^{-7} m/s. The permeability coefficient after reinforcement is reduced by two orders of magnitude, which is consistent with the results of DeJong

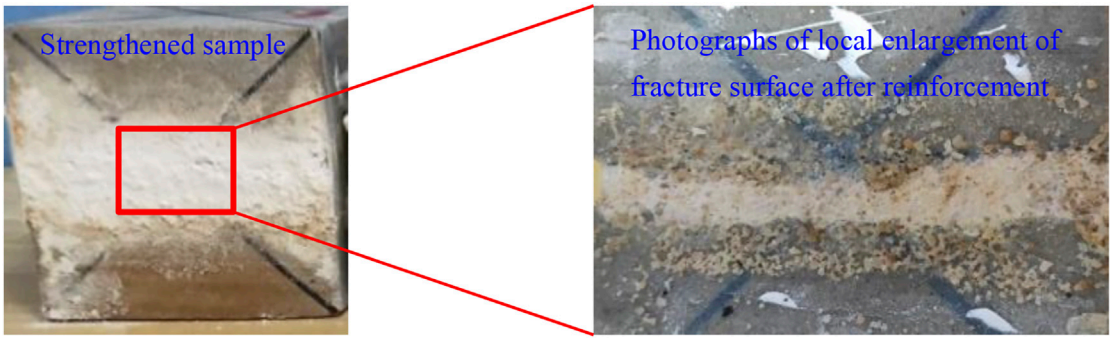

FIGURE 6
Cementing sealing of the fracture surface after reinforcement.

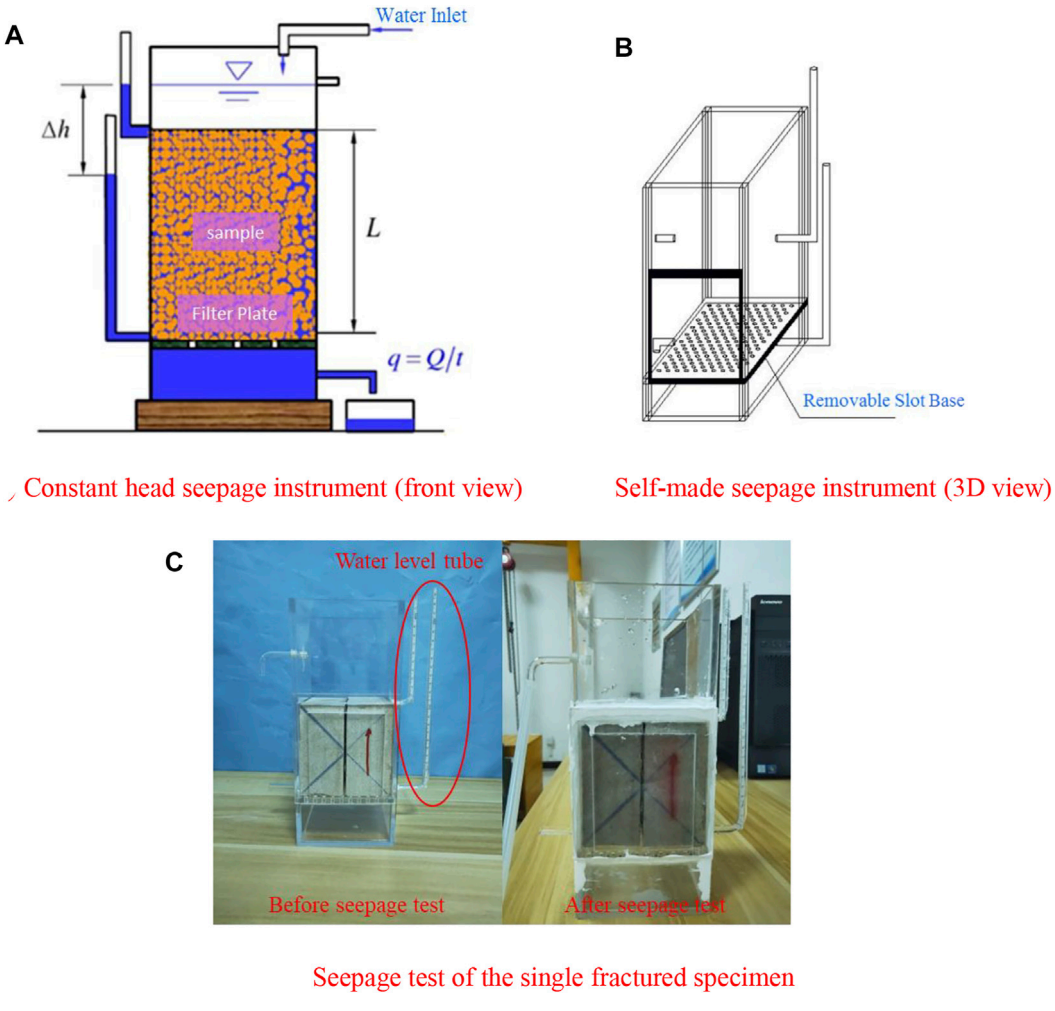

FIGURE 7
Constant head seepage test of the single fractured sample.

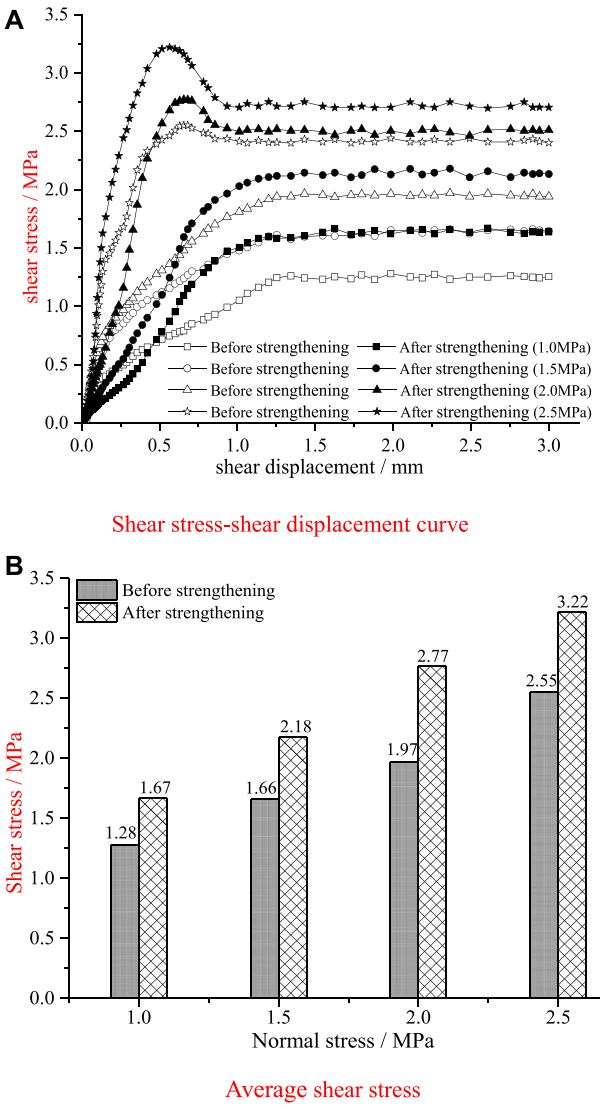

FIGURE 8
Shear stress–shear displacement curve and average shear stress comparison of single fracture samples before and after reinforcement.

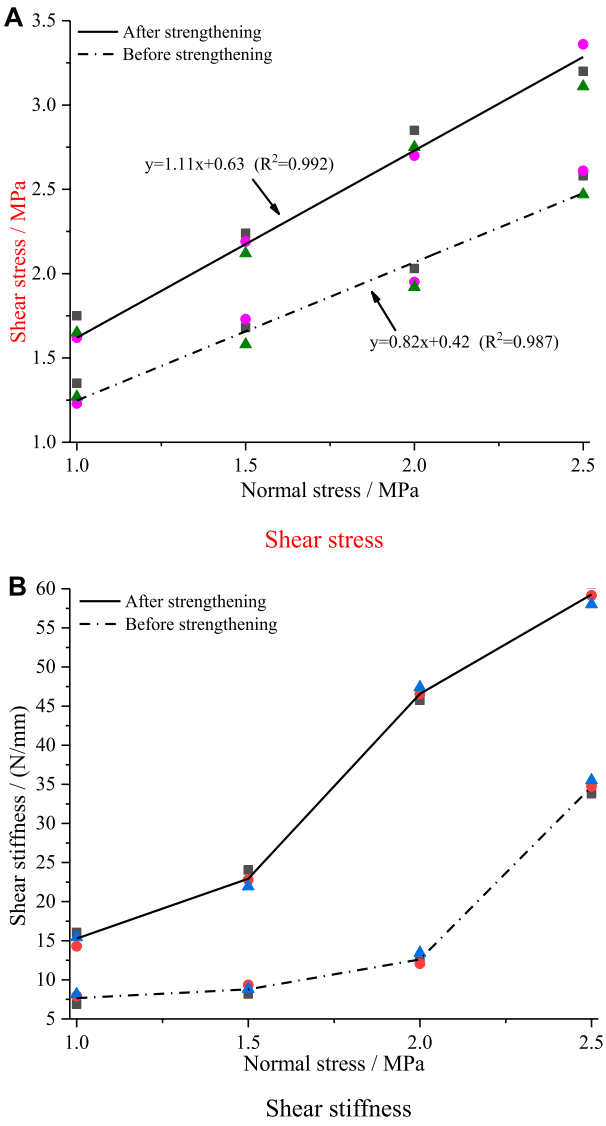

FIGURE 9
Comparison of shear strength parameters and shear stiffness before and after reinforcement.

et al. (2010) and Chu et al. (2012). Due to the filling of standard sand between the fracture surface and the cementation of standard sand and fracture surface by MICP reinforcement, the seepage mode changes from fracture surface seepage to pore seepage, which may be the main reason for the large decrease in the permeability coefficient.

Shear stress

A direct shear test is carried out according to the corresponding samples under different normal stresses during repeated shear tests before reinforcement. The shear stress under different normal stresses is shown in Supplementary Table S2. The comparison of shear stress–shear displacement curves of one group of the samples before and after reinforcement under different normal stresses are shown in Figure 8A. The average value of peak shear stress under different normal stresses is shown in Figure 8B. The shear stress curve with the maximum value is taken as the peak stress. In the curve without obvious peak stress, the shear stress is the strength corresponding to the stable stage.

Before reinforcement, the shear stress–shear displacement curve of the single fractured samples has no obvious peak

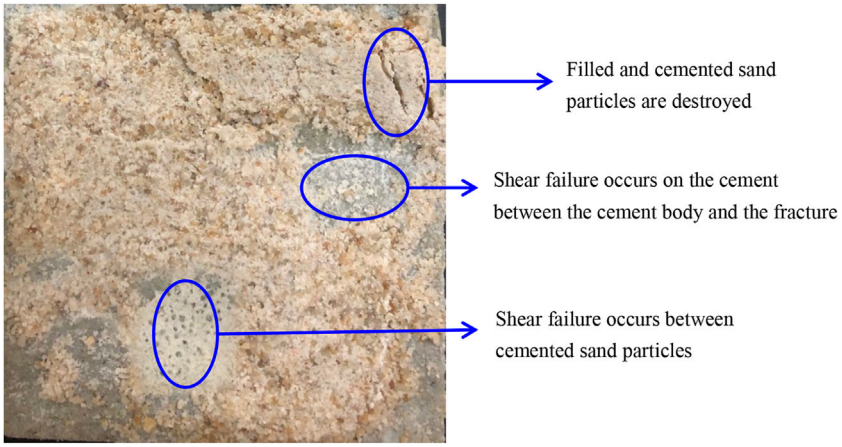

FIGURE 10
Typical shear failure surfaces

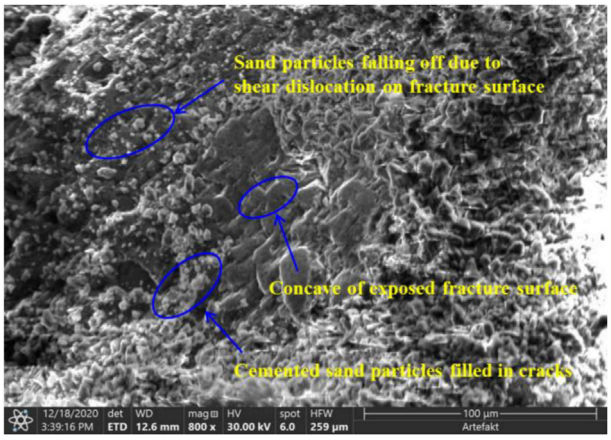

FIGURE 11
SEM comparative analysis of the single fractured sample.

strength stage, and the shear stress increases approximately linearly at the initial stage. With the increase of shear displacement, the slope of the curve gradually decreases until close to the horizontal state, and the curve showed a shear flow state when the shear displacement reached about 1.5 mm. After reinforcement, the shear stress is significantly improved. Under the four normal stresses of 1.0, 1.5, 2.0, and 2.5 MPa, the average shear stress is increased by 30.47, 31.33, 40.61, and 26.27%, respectively. With the increase of normal stress, the peak value of the curve was gradually obvious, and with the increase in shear displacement, there is an obvious stage of residual shear stress. In comparison, the shear stress–shear displacement curves of the samples exhibit obvious change and the shear stress was significantly improved.

According to the Mohr–Coulomb criterion, the average shear stress before and after reinforcement is fitted and analyzed (Figure 9A). It is found that the cohesion of the samples is increased from 0.42 to 0.63 MPa, and the internal friction angle is increased from 39.49° to 47.98°, with an increase of 47.99% and 21.51%, respectively, indicating that MICP technology could effectively improve the shear performance of the single fractured sample and the improvement of the cohesion is particularly obvious.

The shear stiffness under different normal stresses is statistically analyzed (Figure 9B). The average shear stiffness before reinforcement is about 7.66–34.68 N/mm under different normal stresses and then is increased to 15.27–59.27 N/mm after reinforcement, with an increase of 70%–268%, indicating that the shear stiffness is also increased significantly.

Reinforcement mechanism of single fractured sandstone

Typical shear failure surfaces are shown in Figure 10. It can be seen from the graph that there are residual blocks of cement on the failure surface; some shear failure occurs on the cement surface between the cement body and the fracture and some occurs in the cement body. Macroscopically, the shear performance of the fracture surface after MICP reinforcement is significantly improved.

To analyze the reinforcement mechanism of single fractured sandstone, a small piece of the sample after the shear test was taken for SEM scanning, as shown in Figure 11.

It can be seen from the SEM microscopic scanning images that there is a phenomenon by which the filled standard sand falls off and scatters on the fracture surface at the concave part of the

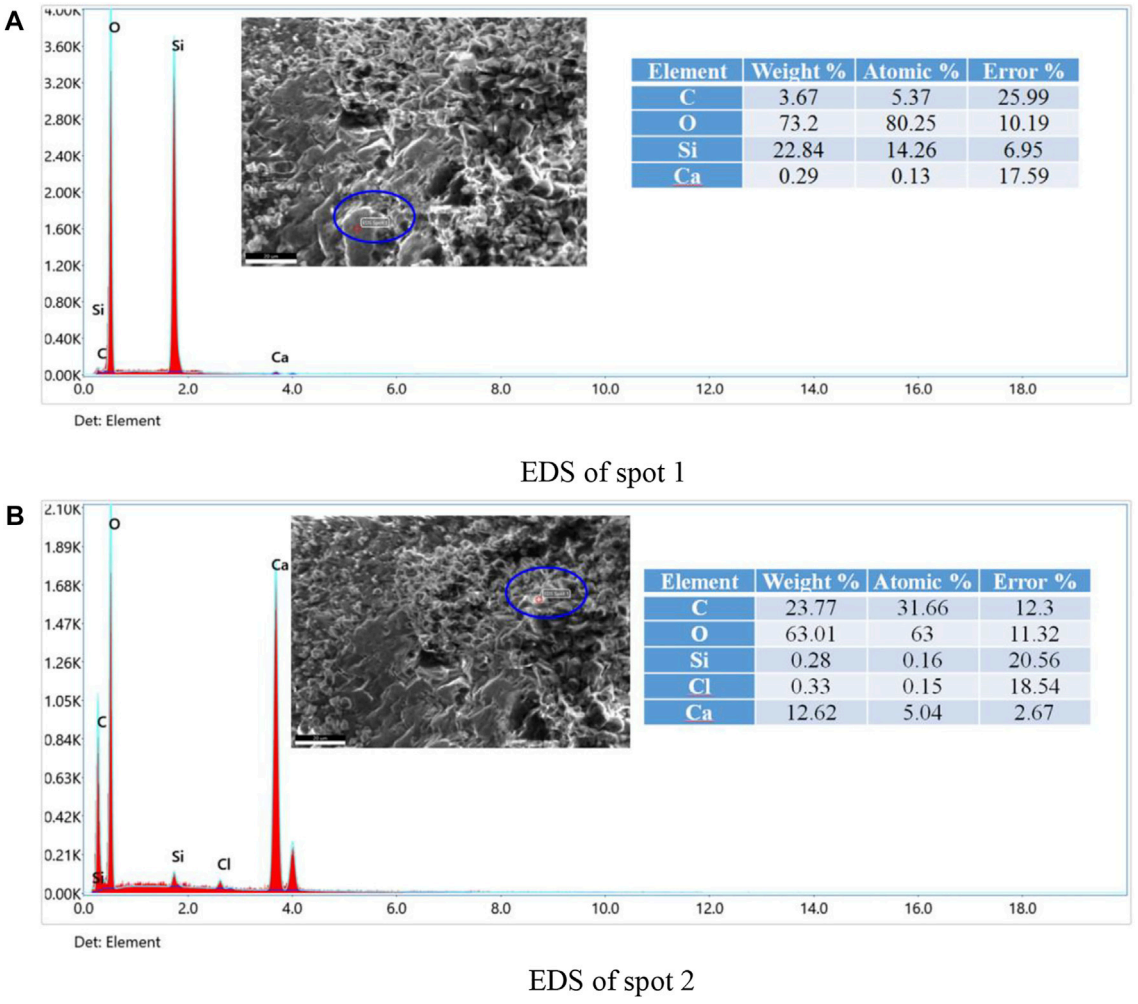

Element	Weight %	Atomic %	Error %
C	3.67	5.37	25.99
O	73.2	80.25	10.19
Si	22.84	14.26	6.95
Ca	0.29	0.13	17.59

Element	Weight %	Atomic %	Error %
C	23.77	31.66	12.3
O	63.01	63	11.32
Si	0.28	0.16	20.56
Cl	0.33	0.15	18.54
Ca	12.62	5.04	2.67

FIGURE 12
EDS comparative analysis of the single fractured sample after reinforcement.

fracture surface after shearing and some sand particles are still cemented on the fracture surface. On the one hand, it indicates that the deposition of calcium carbonate generated by MICP could well cement the sand particles and the fracture surface. On the other hand, it proves that these cemented sites are also locations where shear failure occurs. This further shows that MICP technology has a good reinforcement effect on fractured rock mass.

At the same time, to further analyze the failure mode of cemented filling on the fracture surface caused by shear action, the EDS spectrum of the material on the fracture surface is carried out, as shown in Figure 12.

The chemical components of sandstone are mainly quartz and feldspar. Figure 12A shows that Si and O elements accounted for more than 96% (a small amount of C and Ca elements may be calcium carbonate crystals deposited on the fracture surface), indicating that the material at the detection point is SiO_2. The surface is flat and non-granular, which further indicated that the cemented material is exposed to the sandstone fracture surface after shedding. Figure 12B shows that C, O, and Ca elements accounted for more than 99%, indicating that the detected material is calcium carbonate deposited on the fracture surface.

According to the macroscopic shear failure and microscopic detection analysis, the cementation state of the fracture surface and the failure mode under shear action are analyzed, as shown in Figure 13.

When the single fractured sample is reinforced by microbial grouting, the deposition mode of calcium carbonate with the cementation effect is formed, which is centered on bacteria and calcium carbonate is gathered around it. Macroscopically, a large amount of calcium carbonate is deposited on the fracture surface, sand particles, and between them. With the increase of grouting times, the fracture surface is gradually covered, accumulated, filled, and cemented by the mineralized calcium carbonate. First, for sand

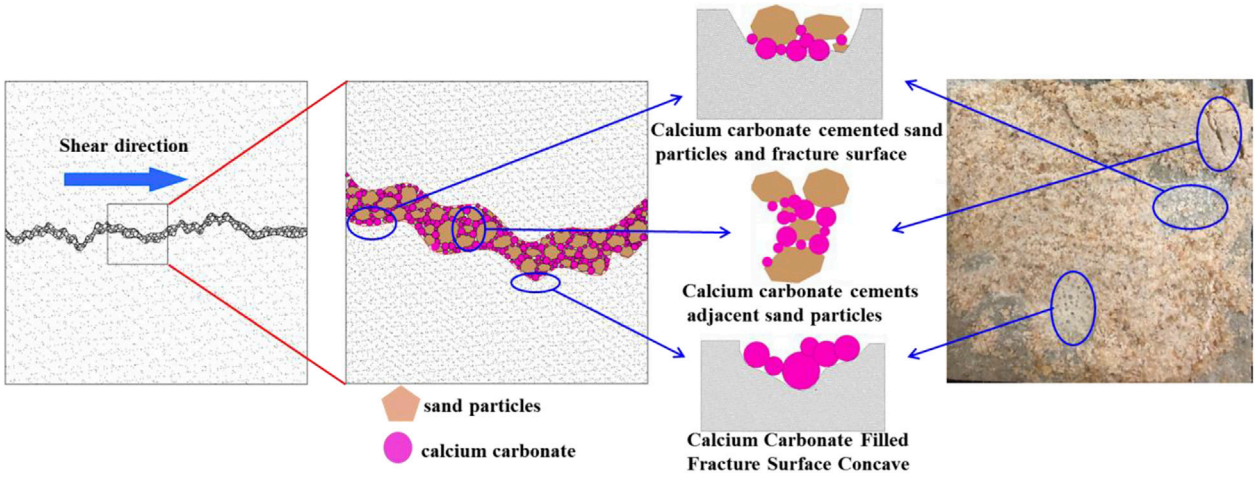

FIGURE 13
Destruction diagram of cemented filling on the fracture surface.

particles, the calcium carbonate produced by the MICP process cements the adjacent sand particles together. After multiple grouting times, the filled sand particles between the fracture surfaces are cemented into a whole. Second, for the fracture surface, the filled sand particles are distributed between the fracture surface and the depression of the fracture surface with an average interval of 1 mm between the upper and lower plates. In the process of grouting, the fracture surface is cemented with the deposited calcium carbonate, and the depression of the fracture surface is filled with calcium carbonate. Therefore, the single fractured sample reinforced by the calcium carbonate generated could be divided into the following three modes of action. First, the calcium carbonate between the sand particles and the fracture surface cements the two together. Second, the calcium carbonate between the sand particles cements the adjacent sand particles. Third, the calcium carbonate in the concave of the fracture surface fills them. These three modes of action form a whole which will cement the upper and lower plates of the fracture rock samples together.

When the fracture surface is damaged by shearing action, the failure mode is the composite failure of the aforementioned three ways of cementation and filling, namely, the failure of the cementation between sand particles and the fracture surface, the failure of the cementation between adjacent sand particles, and the failure of the calcium carbonate filled in the concave of the fracture surface. In this composite failure mode, on the one hand, it shows that the bonding effect between sand particles and the fracture surface and between sand particles improves after reinforcement; on the other hand, calcium carbonate fills in the concave of the fracture surface and cemented the sand particles, and the particle–fracture interaction during the shear test is similar to the shear failure behavior of reinforced concrete (Hu and Wu, 2017; Wu and Hu, 2017). These two aspects jointly improve the performance of the weak surface of the fracture surface, thus improving the strength of the single fractured rock sample after reinforcement.

Conclusion

In this paper, the *in situ* extracted *B. cereus* was used to carry out the experimental study of MICP technology in strengthening fractured rock mass. Through the seepage test and shear test of the samples before and after reinforcement, the improvement effect of MICP technology on the impermeability and shear performance of fractured rock mass was studied. The significance of this study is that we can use environmentally friendly methods to reinforce fractured rock samples, and the impermeability and shear performance after reinforcement have been greatly improved, which provides a certain idea and foundation for the application of this technology to the actual reinforcement project of fractured rock mass. The main conclusions are as follows:

1) The single fractured samples with stable strength are prepared by six times of repeated shear tests before grouting. The permeability of samples before and after reinforcement is tested by a self-made constant head infiltration device and it decreases by two orders of magnitude after reinforcement.
2) After reinforcement, the shear stress of the single fractured samples is increased by 30.47, 31.33, 40.61, and 26.27%, respectively, when the normal stress is 1.0, 1.5, 2.0, and 2.5 MPa. The cohesion increases by 47.99%, and the internal friction angle increases by 21.51%, indicating that *B. cereus* could greatly improve the shear stress of single fractured rock samples, especially in improving the cohesion.

At the same time, the shear stiffness increases significantly after reinforcement, the peak shear strength begins to appear in the shear stress–shear displacement curve, and the residual shear strength is also improved compared with that before reinforcement.

3) SEM scanning shows that the calcium carbonate generated by MICP cements the sand particles with the fracture surface and adjacent sand particles and fills the concave part of the fracture surface. Under the action of the shear test, the three filling states of cementation are destroyed. This composite failure mode also shows that MICP reinforcement technology has a good cementation effect on the fracture surface.
4) Due to the influence of the water level in the Three Gorges Reservoir area with season and water level regulation, the fractured rock mass is in the condition of saturated water and dry circulation for a long time. Therefore, the following research will focus on this engineering feature and conduct several soaking-air drying cycles for MICP-reinforced fractured rock mass to study the change rule of physical and mechanical properties of fractured rock mass under this action, to provide references for the application of this technology in the reinforcement of fractured rock mass.

Data availability statement

The original contributions presented in the study are included in the article/Supplementary Material; further inquiries can be directed to the corresponding author.

Author contributions

XY: conceptualization, data curation, and writing—original draft. DH: methodology, formal analysis, and writing—review and editing. LJ and CX: investigation, supervision, and validation.

Funding

National Natural Science Foundation of China (Project Nos. U2034203, 51979218, 51809151, and 51979151), the Research Fund for Excellent Dissertation of China Three Gorges University (Project No. 2020BSPY001), and the Natural Science Foundation of Hubei Province (Project No. Z2018063).

Conflict of interest

The authors declare that the research was conducted in the absence of any commercial or financial relationships that could be construed as a potential conflict of interest.

Publisher's note

All claims expressed in this article are solely those of the authors and do not necessarily represent those of their affiliated organizations, or those of the publisher, the editors, and the reviewers. Any product that may be evaluated in this article, or claim that may be made by its manufacturer, is not guaranteed or endorsed by the publisher.

Supplementary Material

The Supplementary Material for this article can be found online at: https://www.frontiersin.org/articles/10.3389/feart.2022.905940/full#supplementary-material

References

Ahmed, A. Q., Kenichi, S., and Santamarina, C. (2012). Factors affecting efficiency of microbially induced calcite precipitation. *J. Geotech. Geoenviron* 138 (8), 922–1101. doi:10.1061/(ASCE)GT.1943-5606.0000666

Benmokrane, B., Xu, H. X., and Bellavance, E. (1996). Bond strength of cement grouted glass fibre reinforced plastic (GFRP) anchor bolts. *Int. J. Rock Mech. Min. Sci. Geomechanics Abstr.* 33 (5), 455–465. doi:10.1016/0148-9062(96)00006-X

Chen, F., Deng, C. N., Song, W. J., Zhang, D. Y., Al-Misned, F. A., Mortuza, M. G., et al. (2016). Biostabilization of desert sands using bacterially induced calcite precipitation. *Geomicrobiol. J.* 33 (3-4), 243–249. doi:10.1080/01490451.2015.1053584

Cheng, L., Ralf, C. R., and Mohamed, A. S. (2013). Cementation of sand soil by microbially induced calcite precipitation at various degrees of saturation. *Can. Geotech. J.* 50 (1), 81–90. doi:10.1139/cgj-2012-0023

Chu, J., Stabnikov, V., and Ivanov, V. (2012). Microbially induced calcium carbonate precipitation on surface or in the bulk of soil. *Geomicrobiol. J.* 29 (6), 544–549. doi:10.1080/01490451.2011.592929

Dejong, J. T., Fritzges, M. B., and Nüsslein, K. (2006). Microbially induced cementation to control sand response to undrained shear. *J. Geotech. Geoenviron. Eng.* 132 (11), 1381–1392. doi:10.1061/(ASCE)1090-0241

Dejong, J. T., Mortensen, B. M., Martinez, B. C., and Nelson, D. C. (2010). Bio-mediated soil improvement. *Ecol. Eng.* 36 (2), 197–210. doi:10.1016/j.ecoleng.2008.12.029

Deng, H. F., Xiao, Y., Li, J. L., Duan, L. L., Zhi, Y. Y., and Pan, D. (2018). Degradation laws of joint strength and micro-morphology under repeated shear tests. *Chin. J. Geotechnical Eng.* 40 (2), 183–188. doi:10.11779/CJGE2018S2037

Deng, H. W., Luo, Y. L., Deng, J. R., Wu, L. J., Zhang, Y. N., and Peng, S. W. (2019). Experimental study of improving impermeability and strength of fractured rock by microbial induced carbonate precipitation. *Rock Soil Mech.* 40 (9), 3542–3548. doi:10.16285/j.rsm.2018.0960

Du, Y., Xie, M. W., Jiang, Y. J., Chen, C., Jia, B. N., and Huo, L. C. (2021). Review on the formation mechanism and early warning of rock collapse. *Metal. Mine* 535 (01), 106–119. doi:10.19614/j.cnki.jsks.202101008

Gomez, M. G., Graddy, C. M. R., DeJong, J. T., and Nelson, D. C. (2019). Biogeochemical changes during bio-cementation mediated by stimulated and augmented ureolytic microorganisms. *Sci. Rep.* 9 (1), 11517. doi:10.1038/s41598-019-47973-0

Han, Z. G., Cheng, X. H., and Ma, Q. (2016). An experimental study on dynamic response for MICP strengthening liquefiable sands. *Earthq. Eng. Eng. Vib.* 15 (4), 673–679. doi:10.1007/s11803-016-0357-6

Hu, B., and Wu, Y. F. (2017). Quantification of shear cracking in reinforced concrete beams. *Eng. Struct.* 147, 666–678. doi:10.1016/j.engstruct.2017.06.035

Jiang, N. J., and Soga, K. (2017). The applicability of microbially induced calcite precipitation (MICP) for internal erosion control in gravel-sand mixtures. *Geotechnique* 67 (1), 42–55. doi:10.1680/jgeot.15.P.182

Jiang, Q., Yan, F., Wu, J. Y., Fan, Q. X., Li, S. J., and Xu, D. P. (2019). Grading opening and shearing deformation of deep outward-dip shear belts inside high slope: A case study. *Eng. Geol.* 250, 113–129. doi:10.1016/j.enggeo.2019.01.018

Khan, MdN. H., Amarakoon, G. G. N. N., Shimazaki, S., and Kawasaki, S. (2015). Coral sand solidification test based on microbially induced carbonate precipitation using ureolytic bacteria. *Mat. Trans.* 56 (10), 1725–1732. doi:10.2320/matertrans.M-M2015820

Li, B., Zhang, G. H., Wang, G., and Qiao, J. X. (2022). Damage evolution of frozen-thawed granite based on high-resolution computed tomographic scanning. *Front. Earth Sci. (Lausanne).* 10, 1–12. doi:10.3389/feart.2022.912356

Li, C., Liu, S. H., Zhou, T. J., Gao, Y., and Yao, D. (2017). The strength and porosity properties of MICP-treated aeolian sandy soil. *Mech. Eng.* 39 (2), 165–171+184. doi:10.6052/1000-0879-16-286

Li, C., Wang, S., Wang, Y. X., Gao, Y., and Bai, S. R. G. L. (2019). Field experimental study on stability of bio-mineralization crust in the desert. *Rock Soil Mech.* 40 (4), 1291–1298. doi:10.16285/j.rsm.2018.0677

Li, J. D. (2019). Application of microbial induced calcium carbonate precipitation in reinforcement of fractured rock mass. *Hefei Univ. Technol.* 13, 579. doi:10.27101/d.cnki.ghfgu.2019.000080

Liu, D., Shao, A. L., Li, H., Jin, C. Y., and Li, Y. L. (2020). A study on the enhancement of the mechanical properties of weak structural planes based on microbiologically induced calcium carbonate precipitation. *Bull. Eng. Geol. Environ.* 79 (8), 4349–4362. doi:10.1007/s10064-020-01818-7

Miao, S. J., Wang, H., Cai, M. F., Song, Y. F., and Ma, J. T. (2018). Damage constitutive model and variables of cracked rock in a hydro-chemical environment. *Arab. J. Geosci.* 11 (2), 19. doi:10.1007/s12517-017-3373-6

Montoya, B. M., Dejong, J. T., and Boulanger, R. W. (2013). Dynamic response of liquefiable sand improved by microbial-induced calcite precipitation. *Geotechnique* 63 (4), 302–312. doi:10.1680/geot.SIP13.P.019

Paassen, L. A., Ranajit, G., Thomas, J. M., Star, W. R. L., and van Loosdrecht, M. C. M. (2010). Quantifying biomediated ground improvement by ureolysis: Large-scale biogrout experiment. *J. Geotech. Geoenviron. Eng.* 136 (12), 1721–1728. doi:10.1061/(ASCE)GT.1943-5606.0000382

Qian, C. X., Pan, Q. F., and Wang, R. X. (2010). Cementation of sand grains based on carbonate precipitation induced by microorganism. *Sci. China Technol. Sci.* 53 (8), 2198–2206. doi:10.1007/s11431-009-3189-z

Rong, H., Qian, C. X., and Li, L. Z. (2012). Influence of molding process on mechanical properties of sandstone cemented by microbe cement. *Constr. Build. Mat.* 28 (1), 238–243. doi:10.1016/j.conbuildmat.2011.08.039

Rong, H., Qian, C. X., and Wang, R. X. (2011). A cementation method of loose particles based on microbe-based cement. *Sci. China Technol. Sci.* 54 (7), 1722–1729. doi:10.1007/s11431-011-4408-y

Song, C. P., Elsworth, D., Jia, Y. Z., and Lin, J. Z. (2022). Permeable rock matrix sealed with microbially-induced calcium carbonate precipitation: Evolutions of mechanical behaviors and associated microstructure. *Eng. Geol.* 304, 106697. doi:10.1016/j.enggeo.2022.106697

Tian, K. L., Wu, Y. Y., Zhang, H. L., Li, D., Nie, K. Y., and Zhang, S. C. (2018). Increasing wind erosion resistance of aeolian sandy soil by microbially induced calcium carbonate precipitation. *Land Degrad. Dev.* 29 (12), 4271–4281. doi:10.1002/ldr.3176

Touhidul, Islam. Md., BhaskarChittoori, C. S., and Malcolm, Burbank. (2020). Evaluating the applicability of biostimulated calcium carbonate precipitation to stabilize clayey soils. *J. Mat. Civ. Eng.* 32 (3), 04019369. doi:10.1061/(ASCE)MT.1943-5533.0003036

Wang, S. H., Yang, T. J., Zhang, Z., and Sun, Z. H. 2021. "Unsaturated seepage-stress-damage coupling and dynamic analysis of stability on discrete fractured rock slope." *Environ. Earth Sci.* 80(18), 660. doi:10.1007/s12665-021-09647-x

Whiffin, V. S., Paassen, L. A. V., and Harkes, M. P. (2007). Microbial carbonate precipitation as a soil improvement technique. *Geomicrobiol. J.* 24 (5), 417–423. doi:10.1080/01490450701436505

Wu, Y. F., and Hu, B. 2017. "Shear strength components in reinforced concrete members." *J. Struct. Eng. (N. Y. N. Y).* 143(9), 174–189. doi:10.1061/(ASCE)ST.1943-541X.0001832

Zhang, L., Niu, F. J., Liu, M. H., Ju, X., Wang, Z. W., Wang, J. C., et al. (2022). Fracture characteristics and anisotropic strength criterion of bedded sandstone. *Front. Earth Sci. (Lausanne).* 10, 1–10. doi:10.3389/feart.2022.879332

Zhang, Y., Guo, H. X., and Cheng, X. H. (2015). Role of calcium sources in the strength and microstructure of microbial mortar. *Constr. Build. Mat.* 77, 160–167. doi:10.1016/j.conbuildmat.2014.12.040

Zhao, Q., Li, L., Li, C., Zhang, H. Z., and Amini, F. (2014). A full contact flexible mold for preparing samples based on microbial-induced calcite precipitation technology. *Geotech. Test. J.* 37 (5), 20130090–20130921. doi:10.1520/GTJ20130090

Zhi, Y. Y., Deng, H. F., Xiao, Y., Duan, L. L., Cai, j., and Li, J. L. (2019). Analysis of seepage characteristics of fractured rock mass reinforced by microbial grouting. *Rock Soil Mech.* 40 (1), 1001–1008. doi:10.16285/j.rsm.2018.1708

Zhu, D. P., He, L. A., and Qin, L. K. (2021). Stability of the rock mass reserved in front of anti-slide piles. *KSCE J. Civ. Eng.* 26 (2), 569–583. doi:10.1007/s12205-021-0315-3

Zhu, W. X., Jing, H. W., Yang, L. J., Pan, B., and Su, H. J. (2018). Strength and deformation behaviors of bedded rock mass under bolt reinforcement. *Int. J. Min. Sci. Technol.* 28 (4), 593–599. doi:10.1016/j.ijmst.2018.03.006

Zou, Y. L., Bai, H., Shen, F., Xu, H., and Shou, Y. D. (2021). Experimental investigation on effects of bacterial concentration, crack inclination angle, crack roughness, and crack opening on the fracture permeability using microbially induced carbonate precipitation. *Adv. Civ. Eng.* 2021, 1–15. doi:10.1155/2021/4959229